Influence of Device Geometry on the Non-Volatile Magnetic Flip Flop Characteristics

Thomas Windbacher, Hiwa Mahmoudi, Viktor Sverdlov, and Siegfried Selberherr
Institute for Microelectronics, TU Wien, Gußhausstraße 27–29/E360, A–1040 Wien, Austria
Email: {windbacher | mahmoudi | sverdlov | selberherr}@iue.tuwien.ac.at

***Abstract*—Recently, we proposed a non-volatile magnetic flip flop featuring a very small footprint. We studied its operational limits and current dependent characteristics. Since flip flops are commonly operated by clocked signals, their operation is time critical and the knowledge and understanding of their switching behavior is essential. In this work we study the dependence of the proposed flip flop on its device geometry. In order to facilitate the comparison to the previous results, the same device parameters are employed. The current density was fixed for both inputs at a value of $7 \times 10^{10}\mathrm{A/m^2}$, where all flip flops safely operated, and the free layers' dimensions were varied, independently. The free layer thickness was found as the most critical parameter affecting the switching time, followed by the layer length and a negligible dependence on width.**

I. Introduction

The apparently endless demand for ever more powerful inexpensive electronics made CMOS scaling essential to stay competitive on the semiconductor market. The shrinking of the CMOS devices led to a permanent struggle to keep control over the channel in CMOS devices and caused the introduction of new processes, materials, and device structures e.g. local and global strain techniques, high-k/metal gates, and Tri-gate FETs. At the same time the static power consumption growth and the interconnection delay increase began to grow in importance and state now a significant obstacle for scaling [1]. A simple and elegant solution to get rid of the static power loss is to shut down unused circuit parts entirely and only dissipate power if a read, write, or information procession is required. It is also desired to keep the information in unused circuit parts. This transition towards permanently "Off" circuits entails the introduction of non-volatility and thereby a redesign of all basic building blocks in CMOS. In order to achieve the goal of non-volatile information processing, the use of elements not requiring any power supply in their "Off" state is paramount for a successful implementation.

Spin as a degree of freedom and its exploitation for spin-based devices is very attractive, due to non-volatility, fast operation and high endurance [2]. A plausible and by now commercially available solution to benefit from spintronics is by its exploitation as a supplement and in some cases even as a replacement for static and dynamic CMOS-based memory [3], [4]. The first generation of magnetic random access memory (MRAM) could be read out by the giant magneto-resistance (GMR) or the tunneling magneto-resistance (TMR) [5] effect, but required an additional current carrying wire for writing field generation, which caused high writing energies as well as a disadvantageous scaling behavior and thus hindered its large scale integration applications [6]. The unfavorable writing wire was rendered superfluous by the theoretical prediction

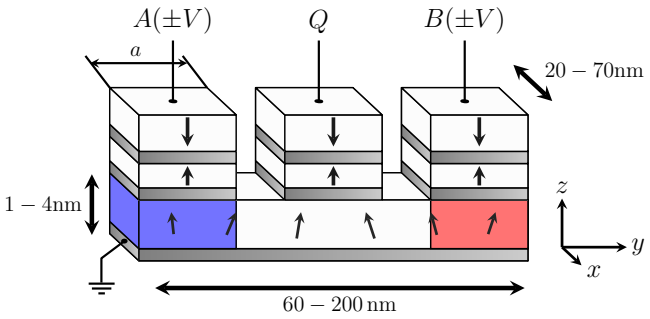

Fig. 1. If two synchronous current pulses are applied at the input stacks A and B, two torques are generated, which either superimpose constructively (current pulses exhibit same polarity and thus same torque orientation) or destructively (current pulses exhibit opposing polarities and thus opposing spin torque orientations). Thus, two sufficiently high and long enough pulses with identical polarity either write logic "0" or "1" into the common free layer, while two pulses with opposing polarities block each other and the initial magnetization state is held.

[7], [8] and experimental proof [9], [10] of the spin transfer torque (STT) effect by enabling a purely electrically controlled switching of magnetic layers. However, there are still challenges to address, like the up to now still rather high current required to switch the magnetization orientation of the free magnetic layer and the decreasing thermal stability when the magnetic tunnel junctions (MTJ) are shrunk. Even though CMOS logic transistors outperform MTJ devices with respect to switching energy [2], the introduction of perpendicular magnetic anisotropies in combination with MgO tunnel barriers reduced the switching energy to a level, where it is able to compete with CMOS SRAM cache [11], [12], [13]. MTJ-based memory technology is especially advantageous with respect to static power loss and already mature enough to encourage the introduction of STT-based MRAM products [4], [14], [15].

Although the combination of MTJs and CMOS transistors seems straight forward and the gained results are very encouraging, the MTJs are normally used as pure memory which only holds the information without further functionality, while the actual information is processed by CMOS transistors [16]. Thus, extra (sense) amplifiers are needed to read and write the non-volatile elements and convert their state into voltage signals. This causes commonly a decrease in integration density, which makes it expensive for large scale integration [17].

II. Idea and Operation Principle

What was said motivated us to investigate alternative solutions which do not require a signal conversion between the magnetic and the CMOS domain and led to the proposal

978-1-4799-5288-5/14/$31.00

Parameter	Value
Free layer length	$60 - 200\text{nm}$
Free layer width	$20 - 90\text{nm}$
Free layer thickness	$1 - 4\text{nm}$
Contact size a	$30\text{nm} \times \text{width}$
Magnetization saturation M_S	$4 \times 10^5 \text{A/m}$
Out-of-plane uni-axial anisotropy K_1	10^5J/m^3
Uniform exchange constant A_{exch}	$2 \times 10^{-11} \text{J/m}$
Polarization P	0.3
Non-magnetic layer	Cu
Gilbert gyromagnetic ratio γ	$2.211 \times 10^5 \text{m/As}$
Damping constant α	0.01
Non-adiabatic contribution ϵ'	0.1 [19]
Fitting parameter Λ	2
Discretization length Δx, Δy	2nm
Discretization length Δz	$1 - 4\text{nm}$
Discretization time Δt	$2 \times 10^{-14} s$

TABLE I. SIMULATION PARAMETERS

of a novel non-volatile magnetic flip flop. The flip flop not only holds the information in the magnetic domain, but also carries out the logic operations via the spin transfer torque effect. Thus, denser and simpler layouts are feasible allowing to simultaneously benefit from the advantageous features related to spintronics [18].

The non-volatile magnetic flip flop comprises three anti-ferromagnetically coupled magnetic polarizer stacks. Two stacks A and B are for input and one stack Q is for readout. All stacks exhibit a perpendicular magnetization and each is connected by a non-magnetic layer (Cu, MgO, Al_2O_3, etc.) to a common free layer with a uni-axial out-of-plane anisotropy K_1 (see Fig. 1). The magnetic orientation of the free layer in relation to the magnetic orientation of the readout stack Q is read either by the GMR or the TMR effect and the apparent high and low resistance states are mapped to logic "0" and "1", respectively.

When a current pulse through one of the input stacks (A or B) is applied, the electrons passing the polarizer stack align to the polarizers magnetization orientation. The polarized electrons enter the free layer, relax to the local free layer orientation, and cause a spin transfer torque acting on the magnetization in the corresponding portion of the free layer (cf. Fig. 1). Depending on the relative orientation between the electrons' polarization vector and the free layer orientation the exerted torque either drives precessions and tries to flip the free layer's magnetization or damps the precessional motions and strives to hold it in its current position.

If now two synchronous current pulses (instead of one) are applied at the input stacks A and B, two spin transfer torques are induced. The two spin transfer torques can point towards the same direction and add up constructively (the current pulses exhibit the same polarity) or they oppose each other and superimpose destructively (the current pulses exhibit opposing polarities). Therefore, two sufficiently long and high enough current pulses with identical polarities RESET/SET the flip flop and two opposing polarities HOLD the free layer orientation. Such a behavior fits perfectly to sequential logic and especially to flip flops. Since flip flops are normally operated by clocked signals, their operation is time critical and the understanding and control of their switching behavior is essential for their utilization.

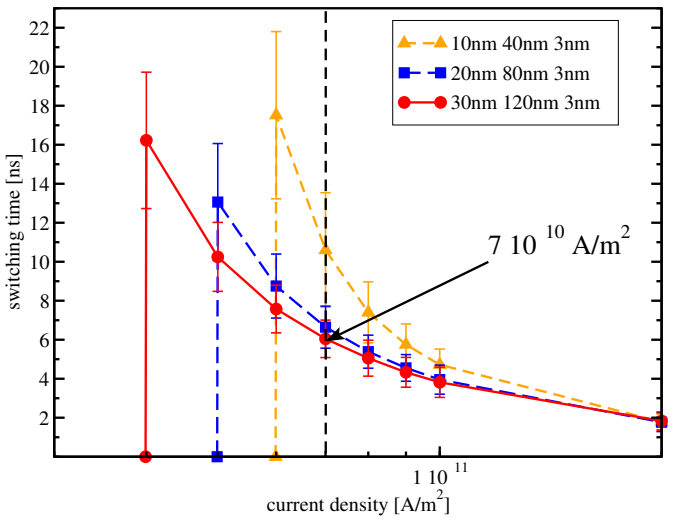

Fig. 2. Switching time as a function of applied current density for two input pulses with identical polarity.

III. SIMULATION SETUP

Before explaining the employed models some basic assumptions and prerequisites must be elucidated. As stated before the non-volatile flip flop exhibits three fixed anti-ferromagnetically coupled polarizer stacks with perpendicular (parallel to the z-axis) magnetization orientation (see Fig. 1). It is contemplated that due to the anti-ferromagnetic nature of the polarizer stacks their stray fields can be neglected. Furthermore, the shared free layer exhibits a constant perpendicular uni-axial anisotropy described by K_1.

The shared free layer dimensions are varied independently, between 20nm and 90nm for the free layer width, between 60nm and 200nm for length, and between 1nm and 4nm for the layer thickness. The applied current density was set within $\pm 5\%$ of 10^7A/m^2 for 101 samples and each layer size in order to allow the averaging of switching times and statistical analysis. The devices' widths are oriented parallel to the x-axis, their lengths along the y-axis, and their thicknesses along the z-axis. The devices are operated by current pulses and the polarity of the pulses is equivalent to logic "0" for negative pulses and "1" for positive pulses.

Assuming a grounded metal layer at the bottom of the free layer and a positive voltage applied to one of the contacts (A, B, or Q) a current flow from the contacts, through the free layer towards the bottom contact will be induced (against the z-axis). This current flow is defined as the positive current direction. At the same time electrons will flow in the opposite direction (positive z-axis).

The simulation parameters were chosen identical to the simulation parameters from [18] to keep the simulation results comparable. All necessary parameters are summarized in Tab. I.

The dynamics of the studied non-volatile magnetic flip flops is governed by the Landau-Lifshitz-Gilbert equation [20], [21] supplemented with an STT term $\vec{T}$:

$$\frac{\mathrm{d}}{\mathrm{d}t}\vec{m} = \gamma \left(-\vec{m} \times \vec{H}_{\text{eff}} + \alpha \left(\vec{m} \times \frac{\mathrm{d}}{\mathrm{d}t}\vec{m} \right) + \vec{T} \right) , \quad (1)$$

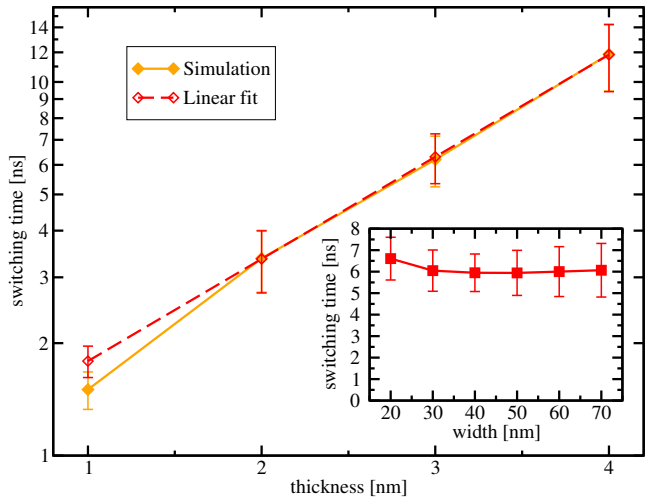

Fig. 3. Logarithmized switching time as a function of free layer thickness. The dashed line shows the linear volume dependence, while the full line depicts our simulation results taking shape anisotropy effects into account. The bars depict the width of the distribution ($\pm 3\sigma$).

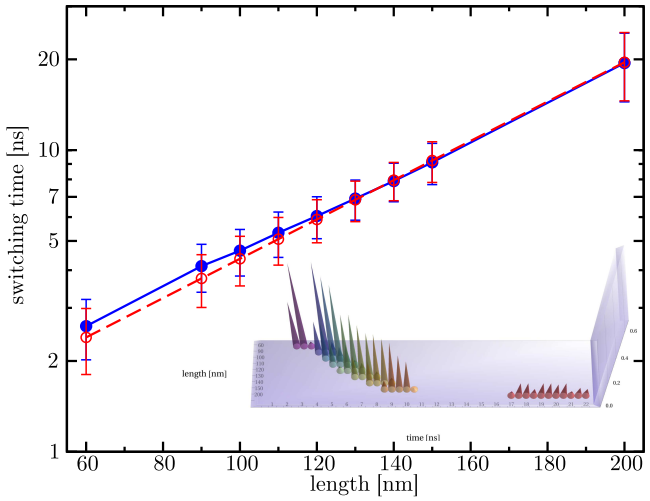

Fig. 4. Logarithmized switching time as a function of free layer length. The dashed line describes the linear energy dependence on the free layer volume (area is fixed). The full line shows our simulation results and deviations due to the shape anisotropy change.

with $\vec{m}$ denoting the reduced magnetization, γ the electron gyromagnetic ratio, α the dimensionless damping constant, and $\vec{H}_{\text{eff}}$ the effective field.

The precessional motion due to the effective magnetic field $\vec{H}_{\text{eff}}$ is described by the first term in (1). A power dissipation proportional to $\frac{\mathrm{d}}{\mathrm{d}t}\vec{m}$ is introduced by the second term and the last term takes care of the spin transfer torque. In the case of non-magnetic layers made out of copper the spin transfer torque $\vec{T}$ is modeled by the following expression [22]:

$$\vec{T} = \frac{\hbar}{\mu_0 e}\frac{J}{l M_S}\frac{P\Lambda^2}{(\Lambda^2+1)+(\Lambda^2-1)\,\vec{m}\cdot\vec{p}} \cdot \\ \cdot\,(\vec{m}\times\vec{p}\times\vec{m}-\epsilon'\vec{m}\times\vec{p})\,. \qquad (2)$$

$\hbar$ denotes the Planck constant, μ_0 the magnetic permeability, J the applied current density, l the free layer thickness, M_S the magnetization saturation, P the spin current polarization, $\vec{p}$ the unit polarization direction of the polarized current, and Λ a fitting parameter handling non-idealities. The STT model for the spin valve exhibits an in-plane ($\vec{m}\times\vec{p}\times\vec{m}$) and a small $\epsilon' \ll 1$ out-of-plane component ($\vec{m}\times\vec{p}$) [19].

The effective field $\vec{H}_{\text{eff}}$ contains contributions from the uni-axial anisotropy, exchange, and demagnetization energy and is gained from the functional derivative of the total free energy density [23].

IV. Results and Discussion

Fig. 3 shows the logarithmized switching time as a function of the free layer thickness. One can immediately see that the free layer thickness has a pronounced influence on the switching time (from $1\text{nm} \rightarrow 1.5\text{ns}$ to $4\text{nm} \rightarrow 11.9\text{ns}$). It can also be observed that for thicker films the linear fit matches very well (linear fit $\rightarrow$ dashed line, simulation data $\rightarrow$ solid line), while for a thickness below 2nm a shorter switching time than predicted by the linear fit is found. In order to explain this behavior we assume an exponential dependence of the switching time $t \propto \exp(E/k_B T)$ [24] on the thermal stability barrier E described by [25]:

$$E = \mu_0/2\, M_S\, V\, (H_{\text{K}_1} - 4\pi N_z M_S)\,. \qquad (3)$$

V describes the free layer volume, H_{K_1} the uni-axial anisotropy field, and N_z the demagnetization factor along the z-axis.

The linear behavior for the thicker free layers is consistent with a saturated demagnetization factor N_z and the linearly growing volume when increasing the layer thickness [25]. On the other hand for thinner free layers the demagnetization factor is not saturated as compared to thick layers and starts to grow when the thickness is decreased. Thus, the difference between the fixed uni-axial anisotropy field H_{K_1} and the growing shape anisotropy [26] becomes smaller which lowers the switching barrier leading to a shorter switching time.

For changing the free layer width (shown in Fig. 3 as inset) the linear volume change is compensated by the linear contact width change and, therefore, the dependence is nearly constant, until the shape anisotropy contribution starts to change significantly and raises the switching barrier (from $20\text{nm} \rightarrow 6.6\text{ns}$ to $70\text{nm} \rightarrow 6\text{ns}$).

The opposite trend shown in Fig. 4 is observed, when the dependence of the switching time on the free layer length is investigated (from $60\text{nm} \rightarrow 2.6\text{ns}$ to $200\text{nm} \rightarrow 19.4\text{ns}$). This is caused by the reduction of N_z for shorter lengths.

The inset of Fig. 4 shows the normalized switching time histograms as a function of the free layer length. Shrinking the volume of the free layer linearly leads to an exponential decrease in switching time [25]. Accordingly, the standard deviation σ, which is defined as the variations from the average, narrows with shrinking free layer volume. A similar trend is shown in Fig. 5, where deviations from the predicted behavior are also caused by the dependence of the shape anisotropy on geometrical parameters.

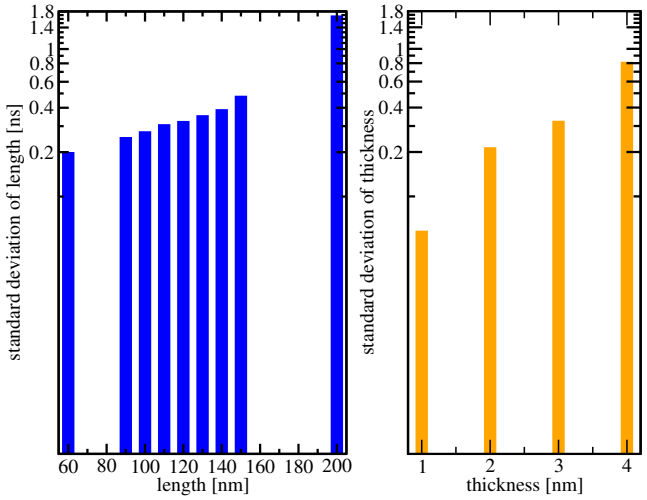

Fig. 5. Standard deviations as a function of length and thickness.

V. Conclusion

The dependence of the switching time of the proposed magnetic flip flop on its device geometry is studied. Changing the free layer thickness and length has a significant influence on the switching time, while changes with respect to width are negligible. This behavior is explained by the exponential dependence of the switching time on the thermal stability barrier and the thermal stability barrier's proportionality to the net anisotropy (out-of-plane anisotropy minus shape anisotropy) times volume. While for the long and broad layers the shape anisotropy contribution is mostly saturated and the (linear) volume dependence dominates, for the short and narrow layers the shape anisotropy starts to depend on the geometrical parameters thus changing the switching barrier and leading to deviations from the linear volume dependence. The weak dependence on changing layer width stems from the counteracting change in contact width which was assumed to be always exactly the same as the device width. Therefore, the free layer thickness is most critical with respect to switching time, followed by the layer length. An additional knob to modulate the switching time is the current density.

Acknowledgment

This work is supported by the European Research Council through the grant #247056 MOSILSPIN.

References

[1] N. Kim et al., "Leakage Current: Moore's Law Meets Static Power," *Computer*, vol. 36, no. 12, pp. 68–75, 2003.

[2] D. Nikonov et al., "Overview of Beyond-CMOS Devices and a Uniform Methodology for Their Benchmarking," *Proceedings of the IEEE*, vol. 101, no. 12, pp. 2498–2533, 2013.

[3] A. Makarov et al., "Emerging Memory Technologies: Trends, Challenges, and Modeling Methods," *Microelectronics Reliability*, vol. 52, no. 4, pp. 628–634, 2012.

[4] Everspin Technologies, Jan. 2014. [Online]. Available: http://www.everspin.com/spinTorqueMRAM.php

[5] S. Ikeda et al., "Tunnel Magnetoresistance of 604% at 300K by Suppression of Ta Diffusion in $CoFeB/MgO/CoFeB$ Pseudo-Spin-Valves Annealed at High Temperature," *Appl. Phys. Lett.*, vol. 93, no. 8, 2008.

[6] C. Chappert et al., "The Emergence of Spin Electronics in Data Storage," *Nat. Mater.*, vol. 6, pp. 813–823, Nov. 2007.

[7] J. Slonczewski, "Current-Driven Excitation of Magnetic Multilayers," *J. Magn. Magn. Mater.*, vol. 159, no. 1–2, pp. L1–L7, 1996.

[8] L. Berger, "Emission of Spin Waves by a Magnetic Multilayer Traversed by a Current," *Phys. Rev. B*, vol. 54, pp. 9353–9358, Oct 1996.

[9] J. S. Moodera et al., "Large Magnetoresistance at Room Temperature in Ferromagnetic Thin Film Tunnel Junctions," *Physical Review Letters*, vol. 74, pp. 3273–3276, Apr. 1995.

[10] T. Miyazaki et al., "Giant Magnetic Tunneling Effect in $Fe/Al_2O_3/Fe$ Junction," *Journal of Magnetism and Magnetic Materials*, vol. 139, no. 3, pp. L231–L234, 1995.

[11] S. Ikeda et al., "A Perpendicular-Anisotropy $CoFeB-MgO$ Magnetic Tunnel Junction," *Nat. Mater.*, vol. 9, pp. 721–724, Sep. 2010.

[12] K. Abe et al., "Novel Hybrid DRAM/MRAM Design for Reducing Power of High Performance Mobile CPU," in *Electron Devices Meeting (IEDM), 2012 IEEE International*, 2012, pp. 10.5.1–10.5.4.

[13] H. Yoda et al., "Progress of STT-MRAM Technology and the Effect on Normally-Off Computing Systems," in *Electron Devices Meeting (IEDM), 2012 IEEE International*, 2012, pp. 11.3.1–11.3.4.

[14] D. Worledge et al., "Materials Advances in Perpendicularly Magnetized MgO-Tunnel Junctions for STT-MRAM," in *Abstracts of the 58th Annual Conference on Magnetism and Magnetic Materials, Symposium on Materials Advances of Spin-Torque Switched Memory Devices for Silicon Integration*, 2013, pp. BA–02.

[15] J. Slaughter et al., "Properties of CMOS-Integrated Magnetic Tunnel Junction Arrays for Spin-Torque Magnetoresistive Random Access Memory," in *Abstracts of the 58th Annual Conference on Magnetism and Magnetic Materials, Symposium on Materials Advances of Spin-Torque Switched Memory Devices for Silicon Integration*, 2013, pp. BA–01.

[16] W. Zhao et al., "Design of MRAM Based Logic Circuits and its Applications," in *ACM Great Lakes Symposium on VLSI*, 2011, pp. 431–436.

[17] K. Rupp et al., "The Economic Limit to Moore's Law," *Semiconductor Manufacturing, IEEE Transactions on*, vol. 24, no. 1, pp. 1–4, Feb 2011.

[18] T. Windbacher et al., "Rigorous Simulation Study of a Novel Non-Volatile Magnetic Flip Flop," in *Proc. of the SISPAD*, 2013, pp. 368–371.

[19] A. V. Khvalkovskiy et al., "High Domain Wall Velocities due to Spin Currents Perpendicular to the Plane," *Phys. Rev. Lett.*, vol. 102, p. 067206, Feb 2009.

[20] T. Gilbert, "A Lagrangian Formulation of the Gyromagnetic Equation of the Magnetization Field." *Phys. Rev.*, vol. 100, p. 1243, 1955.

[21] H. Kronmüller, *Handbook of Magnetism and Advanced Magnetic Materials*. John Wiley & Sons, Ltd, 2007, ch. General Micromagnetic Theory.

[22] J. Xiao et al., "Boltzmann Test of Slonczewski's Theory of Spin-Transfer Torque," *Phys. Rev. B*, vol. 70, p. 172405, Nov 2004.

[23] J. E. Miltat et al., *Handbook of Magnetism and Advanced Magnetic Materials*. John Wiley & Sons, Ltd, 2007, ch. Numerical Micromagnetics: Finite Difference Methods.

[24] J. Harms et al., "SPICE Macromodel of Spin-Torque-Transfer-Operated Magnetic Tunnel Junctions," *Electron Devices, IEEE Transactions on*, vol. 57, no. 6, pp. 1425–1430, June 2010.

[25] R. Sbiaa et al., "Reduction of Switching Current by Spin Transfer Torque Effect in Perpendicular Anisotropy Magnetoresistive Devices," *J.Appl.Phys.*, vol. 109, no. 7, 2011.

[26] A. Aharoni, "Demagnetizing Factors for Rectangular Ferromagnetic Prisms," *J.Appl.Phys.*, vol. 83, no. 6, pp. 3432–3434, 1998.